Effect of Non-Liquefiable High Fines-Content, High Plasticity Soils on Liquefaction Potential Index (LPI) Performance

Sneha Upadhyaya, S.M.ASCE¹; Brett W. Maurer, M.ASCE²; Russell A. Green, P.E., M.ASCE³; and Adrian Rodriguez-Marek, M.ASCE⁴

¹Graduate Student, Dept. of Civil and Environmental Engineering, Virginia Tech, Blacksburg, VA 24061. E-mail: usneha@vt.edu

²Assistant Professor, Dept. of Civil and Environmental Engineering, Univ. of Washington, Seattle, WA 98195. E-mail: bwmaurer@uw.edu

³Professor, Dept. of Civil and Environmental Engineering, Virginia Tech, Blacksburg, VA 24061. E-mail: rugreen@vt.edu

⁴Professor, Dept. of Civil and Environmental Engineering, Virginia Tech, Blacksburg, VA 24061. E-mail: adrainrm@vt.edu

ABSTRACT

The liquefaction potential index (LPI) was found to significantly overpredict the severity of observed liquefaction for a large subset of case histories compiled from Canterbury, New Zealand, earthquakes. One potential cause for these overpredictions is the presence of non-liquefiable capping and interbedded strata with high fines-content and/or plasticity that suppress surficial liquefaction manifestations. Herein, receiver-operating-characteristic analyses of compiled Canterbury, New Zealand, liquefaction case histories are used to investigate LPI performance as a function of the soil-behavior-type index averaged over the upper of 20 m (I_{c20}) of a profile; I_{c20} is used to infer the amount of high fines-content, high-plasticity strata in a profile. It is shown that generally: (1) the relationship between computed LPI and the severity of surficial liquefaction manifestations is I_{c20} -dependent; and (2) the ability of LPI to segregate cases on the basis of observed manifestation severity using LPI decreases with increasing I_{c20} . In conjunction with previous studies, these findings support the need for an improved index that more adequately accounts for the mechanics of liquefaction triggering and manifestation.

INTRODUCTION

The liquefaction potential index (*LPI*) proposed by Iwasaki et al. (1978) is commonly used to characterize the expected severity of liquefaction manifested at the ground surface:

$$LPI = \int_0^{20 \, m} F\left(FS_{liq}\right) \cdot w(z) \, dz \tag{1}$$

where $F(FS_{liq})$ and w(z) are functions that weight the respective influences of FS_{liq} and depth, z, on surface manifestation; and FS_{liq} is the factor of safety against liquefaction triggering, computed by a liquefaction triggering model. Specifically, $F(FS_{liq}) = 1 - FS_{liq}$ for $FS_{liq} \le 1$ and $F(FS_{liq}) = 0$ otherwise; and w(z) = 10 - 0.5z. Thus, LPI assumes that the severity of surface manifestation depends on the cumulative thickness of liquefied strata in a profile's upper 20 m, the proximity of those strata to the ground surface, and the amount by which FS_{liq} in each stratum is less than 1.0. Given this definition, LPI can range from zero to 100. Analyzing data from 55 sites in Japan, Iwasaki et al. (1978) proposed that severe liquefaction is expected for sites where LPI > 15 but not where LPI < 5. This criterion, defined by two threshold values of LPI, is commonly referred to as "Iwasaki Criterion." In today's practice, LPI = 5 is commonly used as a deterministic threshold for predicting surface manifestations, such that some degree of

manifestation is expected where LPI > 5, but no manifestation is expected where LPI < 5.

Despite its popularity, LPI has been found to perform inconsistently in recent earthquakes. For example, LPI was found to significantly overpredict the severity of liquefaction surface manifestations for a large subset of case histories compiled from the 2010-2011 Canterbury Earthquake Sequence (CES) and the 2016 Valentine's Day earthquake in New Zealand (e.g., Maurer et al. 2014; Maurer et al. 2017a). While several factors may contribute to such overpredictions, the presence of interbedded and/or capping non-liquefiable soil strata – in particular, plastic soils with low permeability – may be a significant factor. The presence of such strata can affect the development and redistribution of pore pressure within a soil profile, potentially leading to a suppression of surface manifestations (e.g., Ozutsumi et al. 2002; Juang et al. 2005; Jia and Wang 2012; Maurer et al. 2015a). In this regard, previous studies have shown that the Iwasaki Criterion is less applicable at sites with predominantly silty or clayey soils. For example, Lee et al. (2003) analyzed case histories from the 1999 Chi-Chi (Taiwan) earthquake, mainly comprised of sites with silty sands and sandy silt strata, and proposed that a threshold LPI of 13 should be used to distinguish between sites with and without manifestations of liquefaction (in contrast with the LPI = 5 threshold commonly used in practice). Similarly, Maurer et al. (2015a) found this threshold LPI value to be significantly higher at sites with predominantly silty and clayey soil mixtures than at sites with predominantly clean sands or silty sands. Maurer et al. (2015a) made this distinction using the Cone Penetration Test (CPT) soil-behavior-type index (I_c) developed by Robertson and Wride (1998) to compute an average I_c for the uppermost 10 m of each soil profile (I_{c10}) . Sites were then parsed into those comprised of predominantly clean sands or silty sands ($I_{c10} < 2.05$), and those comprised of predominantly silty or clayey soil mixtures ($I_{c10} \ge 2.05$). Most importantly, they found that sites with $I_{c10} < 2.05$ had an optimum threshold LPI of 4.0 whereas sites with $I_{cI0} \ge 2.05$ had an optimum threshold LPI of 13. From these studies, it can be inferred that the relationship between computed LPI and the severity of liquefaction surface-manifestation is dependent on the stratification and soil properties of nonliquefiable layers, in addition to those of liquefiable strata, which LPI already considers (see Eq. 1).

Accordingly, the objective of this study is to rigorously investigate the effect of non-liquefiable high fines-content, high plasticity soils on LPI performance. Using an approach similar to Maurer et al. (2015a), this study uses the I_c averaged over a depth of 20 m, herein referred to as I_{c20} , to parse soil profiles by their average inferred soil-type. The depth of 20 m was chosen based on the maximum depth that LPI considers, but a future study will evaluate the significance of this consideration. The present study improves on prior research in that it: (1) evaluates 9260 case histories, significantly more than in past studies; (2) parses case histories into finer I_{c20} bins, such that the influence of I_{c20} on LPI performance can be studied in greater resolution; and (3) investigates the influence of I_{c20} on LPI's ability to predict not only manifestations of any severity (as was done previously), but also to predict particular severities of manifestations, as classified using the Green et al. (2014) criteria: marginal manifestations; moderate manifestations; and severe manifestations. The long-term goal of this work is to improve LPI performance by understanding and incorporating the influence of non-liquefiable high fines-content, high plasticity soils on liquefaction hazard.

DATA AND METHODOLOGY

This study utilizes about 3500 CPT soundings from sites where the severity of liquefaction was well-documented after at least one of the following earthquakes: the M_w 7.1 September 2010

Darfield earthquake; the M_w 6.2 February 2011 Christchurch earthquake; and the M_w 5.7 February 2016 Valentine's Day earthquake, collectively referred to herein as the Canterbury earthquakes (CE), resulting in 9260 high quality liquefaction case histories. A detailed description of the selection/rejection criteria for the CPT soundings is provided in Maurer et al. (2014, 2015a). The severity of liquefaction manifested at the ground surface was classified in accordance with Green et al. (2014) via post-earthquake ground reconnaissance and using high-resolution aerial and satellite imagery. The CPT soundings and imagery used in this study were extracted from the New Zealand Geotechnical Database (NZGD 2016).

The estimation of peak ground acceleration (PGA) is required to compute FS_{liq} and was made following the Bradley (2013) procedure, which has been used in many prior CE studies, including Green et al. (2011, 2014) and Maurer et al. (2014, 2015a,b) among others. The depth of ground water table immediately prior to each earthquake was estimated using the event-specific regional ground water models of van Ballegooy et al. (2014). FS_{liq} was computed using the Boulanger and Idriss (2014) deterministic liquefaction triggering model. Inherent to this process, an I_c cutoff value of 2.6 was used to distinguish between liquefiable and non-liquefiable soils, such that soils with $I_c > 2.6$ were considered to be non-liquefiable. Finally, LPI was computed for each of the 9260 case histories considered in this study.

To study the effect of non-liquefiable high fines-content, high plasticity soils on LPI performance, the case history sites were divided into five subsets on the basis of I_{c20} , wherein I_{c20} is used to infer the extent to which a profile contains high fines-content, high-plasticity soils. The use of I_c for inferring soil type was first proposed by Jeffries and Davies (1993) and then modified and popularized by Robertson and Wride (1998). Using CPT data and lab tests on samples from parallel borings, Maurer et al. (2017b) confirmed the suitability of using I_c to infer fines content and soil type within the CE study area.

Receiver-operating-characteristic (ROC) analyses (e.g., Fawcett 2005) were then performed on each I_{c20} subset to evaluate the extent to which two aspects of LPI performance are I_{c20} -dependent: (1) the relationship between computed LPI and the severity of liquefaction surface-manifestation; and (2) the efficiency of LPI predictions (i.e., the ability to use LPI to segregate cases based on observed manifestation severity). The use of ROC analyses for evaluating these aspects of LPI performance is briefly summarized in the following section.

Overview of ROC Analyses

ROC analyses are commonly used to evaluate the performance of diagnostic models and have been used extensively in medical diagnostics (e.g., Zou 2007) and to a much lesser degree in geotechnical engineering (e.g., Oommen et al. 2010; Maurer et al. 2015a, 2017a,b,c; Green et al. 2017; Zhu et al. 2017). In particular, ROC analyses can be used (1) to identify the optimum diagnostic thresholds (e.g., *LPI* values) for distinguishing between classification subsets (e.g., cases with and without manifestations of liquefaction); and (2) to assess the efficiency with which those optimum thresholds operate (e.g., how well does *LPI* = 5 separate cases with and without manifestations?).

In any ROC analysis application, the distribution of "positives" (e.g., cases of observed surficial liquefaction manifestations) and "negatives" (e.g., cases of no observed surficial liquefaction manifestations) overlap when the frequency of the distributions are expressed as a function of the diagnostic test results (e.g., LPI values). A ROC curve can be drawn by plotting the True Positive Rate (R_{TP}) (e.g., liquefaction is predicted and manifestations were observed) versus the False Positive Rate (R_{FP}) (e.g., liquefaction is predicted but no manifestations were

observed) for varying threshold values (e.g., threshold *LPI* values). A conceptual illustration of ROC analysis, including the relationship among the positive and negative distributions, the threshold value, and the ROC curve, is shown in Figure 1.

In ROC curve space, a random guess is indicated by 1:1 line through the origin, while a perfect model plots along the left vertical and upper horizontal axes, connecting at a point (0,1). A perfect model indicates the existence of a threshold value that perfectly segregates the dataset (e.g., a threshold LPI value below which all the cases are "no manifestation" and above which all the cases are "manifestation"). The area under the ROC curve (AUC) can be used as a metric to evaluate the predictive performance of a diagnostic test (e.g., LPI) whereby higher AUC indicates better predictive capabilities. AUC is statistically equivalent to the probability that sites observed to have liquefaction surface manifestations have higher LPI values than sites observed to have no surface manifestations (Fawcett 2005). As such, a random guess returns an AUC of 0.5 whereas a perfect model returns an AUC of 1. The optimum operating point (OOP) is the optimal threshold value that minimizes the rate of misprediction [i.e., $R_{FP} + (1-R_{TP})$]. Contours of the quantity $[R_{FP} + (1-R_{TP})]$ are iso-performance lines joining points of equivalent performance in ROC space, as illustrated in Figure 1b.

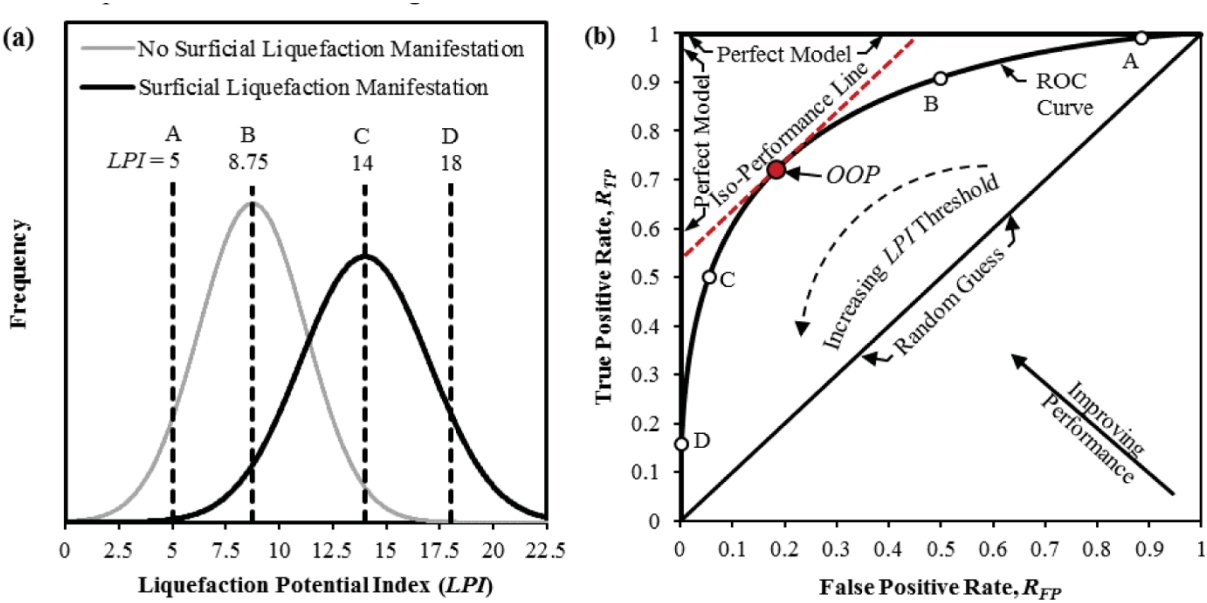


Figure 1. Conceptual illustration of ROC analyses: (a) frequency distributions of liquefaction manifestation and no liquefaction manifestation observations as a function of *LPI*; (b) corresponding ROC curve, and illustration of how a ROC curve is used to assess the efficiency of a diagnostic test (after Maurer et al. 2015a,b).

RESULTS AND DISCUSSION

Figure 2 shows the plot of LPI versus I_{c20} for all CE case studies considered. ROC analyses were performed on subsets of this data, formed by grouping the database into different bins of I_{c20} , and the corresponding AUC and OOP were obtained for each bin, considering also the classification of observed manifestation severity. Initially, the database was divided into two groups of I_{c20} : $I_{c20} < 2.05$ and $I_{c20} \ge 2.05$, where $I_c = 2.05$ is the I_c boundary between clean sands to silty sands and silty sands to sandy silts (Robertson and Wride 1998). ROC statistics were obtained to evaluate the performance of LPI in distinguishing (a) cases with no manifestation

from cases with any manifestation; (b) cases with no manifestation from cases with either moderate or severe manifestations (i.e., excluding marginal manifestations); (c) cases with no manifestation from cases with marginal manifestation; (d) cases with marginal manifestation from cases with moderate manifestation; and e) cases with moderate manifestation from cases with severe manifestation. Table 1 summarizes *AUC* and *OOP* values for each of the above.

In general, the *OOP* values for the subset of cases with $I_{c20} \ge 2.05$ are significantly higher than those for the subset with $I_{c20} < 2.05$, indicating that the relationship between LPI and manifestation severity varies with I_{c20} . In addition, the AUC values for $I_{c20} < 2.05$ were found to be generally higher than those for $I_{c20} \ge 2.05$, indicating that LPI is better at distinguishing between cases with different manifestation severity at sites with $I_{c20} < 2.05$. It can also be observed that LPI is more efficient in predicting the manifestation of surficial liquefaction features than in predicting the severity of manifestation (e.g., distinguishing between marginal versus moderate manifestations), as indicated by the corresponding AUC values.

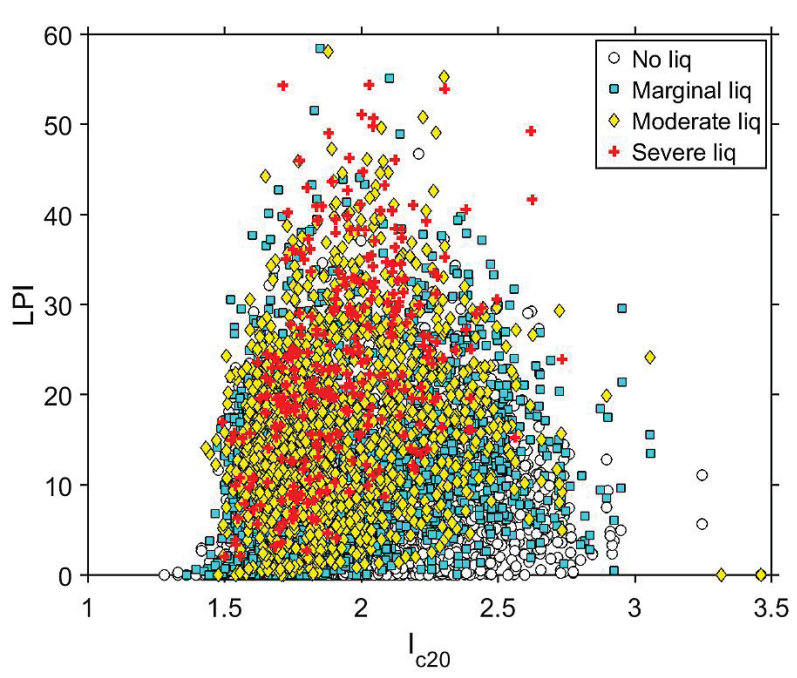


Figure 2. LPI versus I_{c20} , parsed by the observed severity of liquefaction manifestation.

Table 1. Summary of ROC analyses on two subsets of $I_{c2\theta}$ for different classifications of observed liquefaction surface manifestation; codes (a) through (e) are described in the text.

Dataset assessed	All Severities (a)		Moderate and Severe (b)		Marginal (c)		Moderate (d)		Severe (e)	
	AUC	OOP	AUC	OOP	AUC	OOP	AUC	OOP	AUC	OOP
$I_{c20} < 2.05$	0.878	4.60	0.940	5.70	0.821	3.70	0.693	10.40	0.681	19.60
$I_{c20} \ge 2.05$	0.770	11.50	0.838	13.40	0.731	9.30	0.609	14.20	0.740	19.30

Similar analyses were performed using finer bins of I_{c20} to evaluate the influence of I_{c20} on *LPI* performance in greater resolution. Table 2 summarizes *AUC* and *OOP* values, binned by I_{c20} ,

which describe the performance of LPI in distinguishing between several classifications of observed manifestation severity, as described previously. In general, the optimum threshold LPI values increase with increasing I_{c20} for all classifications of observed manifestation severity. This clearly indicates that the relationship between computed LPI and the severity of surficial liquefaction manifestations is I_{c20} -dependent, such that for a given LPI value, the severity of manifestation decreases as I_{c20} increases. For example, the optimum LPI threshold for distinguishing cases with no manifestation from cases with manifestations of any severity is 4.6 for cases with $1.7 \le I_{c20} < 1.9$. In contrast, this threshold is 14.6 for cases with $I_{c20} \ge 2.3$. Thus, the appropriateness of the commonly-used Iwasaki Criterion is very much a function of I_{c20} – the results of this study strongly suggest that it should not be used at sites with high I_{c20} . This is notable considering that the Iwasaki Criterion has been used worldwide since its inception.

Moreover, it can be observed that AUC values generally decrease with increasing I_{c20} , indicating that the efficiency of the optimum LPI thresholds in Table 2 (i.e., the ability to segregate cases based on observed manifestation severity using LPI thresholds) decreases with increasing I_{c20} . Collectively, these results suggest that LPI is prone to performing poorly as I_{c20} increases. It should be noted that in the case of distinguishing between moderate and severe manifestations, the opposite trend between AUC and I_{c20} was seen, whereby AUC increased with increasing I_{c20} . One reason for this inconsistency could be the varying robustness of the case histories in the I_{c20} bins. In particular, "severe manifestation" cases are the least numerous in the database.

Table 2. Summary of ROC analyses on subsets of smaller $I_{c2\theta}$ bins for different cases of liquefaction surface manifestation.

Dataset assessed	Any (a)		Moderate & Severe (b)		Marginal (c)		Moderate (d)		Severe (e)	
	AUC	OOP	AUC	OOP	AUC	OOP	AUC	OOP	AUC	OOP
I_{c20} < 1.7	0.888	3.7	0.951	4.8	0.842	3.6	0.670	5.2	0.510	15.0
$1.7 \le I_{c2\theta} < 1.9$	0.881	4.6	0.940	6.2	0.822	3.7	0.702	10.4	0.672	18.7
$1.9 \le I_{c2\theta} < 2.1$	0.831	8.5	0.907	9.1	0.747	8.2	0.699	14.0	0.718	19.8
$2.1 \le I_{c2\theta} < 2.3$	0.803	10.0	0.852	10.2	0.768	9.9	0.573	14.2	0.740	24.2
$I_{c2\theta} \geq 2.3$	0.716	14.6	0.784	14.9	0.690	11.5	0.589	14.9	0.783	24.0

CONCLUSION

Using 9,260 liquefaction case histories compiled from the Canterbury earthquakes, this study investigated LPI performance as a function of the soil-behavior-type index averaged over a depth of 20 m (I_{c20}), wherein I_{c20} was used to infer the extent to which a profile contains high finescontent, high-plasticity soils. It was shown that generally: (1) the relationship between computed LPI and the severity of liquefaction surface-manifestation is I_{c20} -dependent, such that at any given LPI value, the severity of manifestation decreases as I_{c20} increases; and (2) the efficiency of LPI predictions (i.e., the ability to segregate cases based on observed manifestation severity using LPI thresholds) decreases with increasing I_{c20} , indicating that LPI is prone to performing

poorly as I_{c20} increases. Collectively, these findings suggest that I_{c20} -specific threshold LPI values may be needed to accurately assess liquefaction hazard using LPI, but that when I_{c20} is high, LPI is unlikely to efficiently predict the severity of manifestations, even if I_{c20} -specific thresholds are employed. Finally, the results from this study are entirely based on a database from the 2010-2011 and 2016 Canterbury, New Zealand, earthquakes; the applicability of these findings to other datasets is unknown.

ACKNOWLEDGEMENTS

This research was funded by National Science Foundation (NSF) grants CMMI-1030564, CMMI-1435494, and CMMI-1724575. However, any opinions, findings, and conclusions or recommendations expressed in this paper are those of the authors and do not necessarily reflect the views of NSF.

REFERENCES

- Boulanger, R.W. and Idriss, I.M. (2014). *CPT and SPT based liquefaction triggering procedures*. Report No. UCD/CGM.-14/01, Center for Geotechnical Modelling, Department of Civil and Environmental Engineering, UC Davis, CA, U.S.
- Bradley, B.A. (2013). "Site-Specific and spatially-distributed ground motion intensity estimation in the 2010-2011 Christchurch earthquakes." *Soil Dynamics and Earthquake Engineering*, 48, 35-47.
- Fawcett, T. (2006). "An introduction to ROC analysis." *Pattern recognition letters*, 27(8), 861-874.
- Green, R.A., Allen, J., Wotherspoon, L., Cubrinovski, M., Bradley, B., Bradshaw, A., Cox, B., and Algie, T. (2011). "Performance of levees (stopbanks) during the 4 September 2010, M_w7.1 Darfield and 22 February 2011, M_w6.2 Christchurch, New Zealand earthquakes," *Seismological Research Letters*, 82(6), 939-949.
- Green, R.A., Cubrinovski, M., Cox, B., Wood, C., Wotherspoon, L., Bradley, B., and Maurer, B.W. (2014). "Select liquefaction case histories from the 2010-2011 Canterbury earthquake sequence." *Earthquake Spectra*, 30(1), 131-153.
- Green, R.A., Upadhyaya, S., Wood, C.M., Maurer, B.W., Cox, B.R., Wotherspoon, L., Bradley, B.A., and Cubrinovski M. (2017). "Relative efficacy of CPT- versus Vs-based simplified liquefaction evaluation procedures," *Proc.* 19th Intern. Conf. on Soil Mechanics and Geotechnical Engineering, Seoul, Korea, 17-22 September.
- Iwasaki, T., Tatsuoka, F., Tokida, K., & Yasuda, S. (1978). "A practical method for assessing soil liquefaction potential based on case studies at various sites in Japan." *Proceedings of the 2nd International Conference on Microzonation*, Nov 26-Dec 1, San Francisco, CA, U.S.
- Jia, M.C. and Wang, B.Y. (2012). "Liquefaction testing of stratified sands interlayered with silt." *Applied Mechanics and Materials*, 256, 116-119.
- Juang, C. H., Yang, S. H., Yuan, H., and FANG, S. Y. (2005). "Liquefaction in the Chi-Chi earthquake-effect of fines and capping non-liquefiable layers." *Soils and Foundations*, 45(6), 89-101.
- Lee, D.H., Ku, C.S., and Yuan, H. (2003). "A study of liquefaction risk potential at Yuanlin, Taiwan." *Engineering Geology*, 71(1), 97-117.
- Maurer, B.W., Green, R.A., Cubrinovski, M., and Bradley, B.A. (2014). "Evaluation of the liquefaction potential index for assessing liquefaction hazard in Christchurch, New Zealand." *Journal of Geotechnical and Geoenvironmental Engineering*, 140(7): 04014032.

- Maurer, B.W., Green, R.A., Cubrinovski, M., and Bradley, B. (2015a). "Fines-content effects on liquefaction hazard evaluation for infrastructure during the 2010-2011 Canterbury, New Zealand earthquake sequence." *Soil Dynamics and Earthquake Engineering*, 76, 58-68.
- Maurer, B.W., Green, R.A., Cubrinovski, M., and Bradley, B. (2015b). "Assessment of CPT-based methods for liquefaction evaluation in a liquefaction potential index framework." *Géotechnique* 65(5), 328-336.
- Maurer, B.W., Green, R.A., van Ballegooy, S., Bradley, B.A., and Upadhyaya, S. (2017a). "Performance comparison of probabilistic and deterministic liquefaction triggering models for hazard assessment in 23 global earthquakes." *Geo-Risk 2017: Reliability-based design and code developments* (J. Huang, G.A. Fenton, L. Zhang, and D.V. Griffiths, eds.), ASCE Geotechnical Special Publication 283, 31-42.
- Maurer, B.W., Green, R.A., van Ballegooy, S., and Wotherspoon, L. (2017b). "Development of region-specific soil behavior type index correlations for evaluating liquefaction hazard in Christchurch, New Zealand." *Soil Dynamics and Earthquake Engineering*, (*In Review*).
- Maurer, B.W., Green, R.A., van Ballegooy, S., and Wotherspoon, L. (2017c). "Assessing liquefaction susceptibility using the CPT Soil Behavior Type Index," *Proc.* 3rd Intern. Conf. on Performance-Based Design in Earthquake Geotechnical Engineering (PBDIII), Vancouver, Canada, 16-19 July.
- NZGD (2016). *New Zealand Geotechnical Database*. https://www.nzgd.org.nz/Default.aspx Accessed 8/24/16. New Zealand Earthquake Commission (EQC).
- Oommen, T., Baise, L. G., and Vogel, R. (2010). "Validation and application of empirical liquefaction models." *Journal of Geotechnical and Geoenvironmental Engineering*, 136(12), 1618-1633.
- Ozutsumi, O., Sawada, S., Iai, S., Takeshima, Y., Sugiyama, W., and Shimazu, T. (2002). "Effective stress analyses of liquefaction-induced deformation in river dikes." *Soil Dynamics and Earthquake Engineering*, 22(9), 1075-1082.
- Robertson, P.K. and Wride, C.E. (1998). "Evaluating cyclic liquefaction potential using cone penetration test." *Canadian Geotechnical Journal*, 35(3), 442-459.
- van Ballegooy, S., Cox, S.C., Thurlow, C., Rutter, H.K., Reynolds, T., Harrington, G., Fraser, J., and Smith, T. (2014). *Median water table elevation in Christchurch and surrounding area after the 4 September 2010 Darfield earthquake: Version 2.* GNS Science Report 2014/18.
- Zhu, J., Baise, L.G., and Thompson, E.M. (2017). "An updated geospatial liquefaction model for global application." *Bulletin of the Seismological Society of America*, 107(3), doi: 10.1785/0120160198
- Zou, K.H. (2007). "Receiver operating characteristic (ROC) literature research." On-line bibliography available from: http://www.spl.harvard.edu/archive/spl-pre2007/pages/ppl/zou/roc.html accessed 10 March 2016.